Heteroatom Chemistry
Volume 8, Number 6, 1997

Theoretical Study of the Mechanism of the Wittig Reaction: Ab Initio and MNDO-PM3 Treatment of the Reaction of Unstabilized, Semistabilized and Stabilized Ylides with Acetaldehyde[1]

Albeiro A. Restrepo-Cossio, Hermisul Cano, and Frank Marí*

Department of Chemistry and Biochemistry, Florida Atlantic University, 777 Glades Rd., Boca Raton, Florida 33431

Carlos A. Gonzalez†

Pittsburgh Supercomputing Center, Carnegie Mellon University, 4400 Fifth Ave., Pittsburgh, Pennsylvania 15213

Received 3 July 1997; revised 31 July 1997

ABSTRACT

In this study, we describe the results of ab initio (HF and MP2) and MNDO-PM3 calculations on the model reactions of unstabilized ($Me_3P{=}CH{-}CH_3$), semistabilized ($Me_3P{=}CH{-}C{\equiv}CH$), and stabilized ($Me_3P{=}CH{-}C{\equiv}N$) ylides with acetaldehyde to form their respective Z and E olefins and trimethylphosphine oxide. These reactions occur in three stages: oxaphosphetane formation, oxaphosphetane pseudorotation, and oxaphosphetane decomposition. The calculated barriers for these processes vary considerably depending on the level of theory employed (ab initio vs. MNDO-PM3 or HF vs. MP2 at the ab initio level). However, self-consistent geometries of reactants, intermediates, transition states and products are obtained at all levels. Oxaphosphetane formation is best described as very asynchronous cycloaddition (borderline two-step mechanisms). The geometries of the transition states are near planar with respect to P, C, C, and O atoms. Analysis of the bond indices of these reactions shows that the C–C bonds are between 44% (unstabilized case) and 60% (stabilized case) formed, whereas the corresponding P–O bonds have not been formed to any significant degree. Oxaphosphetane decomposition can be described as a very asynchronous retrocycloaddition where P–C bond breakage runs ahead of C–O bond breakage. These results are compared with experimental findings for the Wittig reaction, and its relevance to the overall mechanism of the olefination is discussed. © 1997 John Wiley & Sons, Inc. Heteroatom Chem **8**:557–569, 1997

INTRODUCTION

The Wittig olefination reaction is one of the most important methods in synthetic organic chemistry (Scheme 1) [2]. This reaction involves the nucleo-

---

Dedicated to Prof. William E. McEwen on the occasion of his seventy-fifth birthday.

*To whom correspondence should be addressed.

†Current address: Physical and Chemical Properties Division, Blg 221, National Institute of Standards and Technology, Gaithersburg, MD 20899.

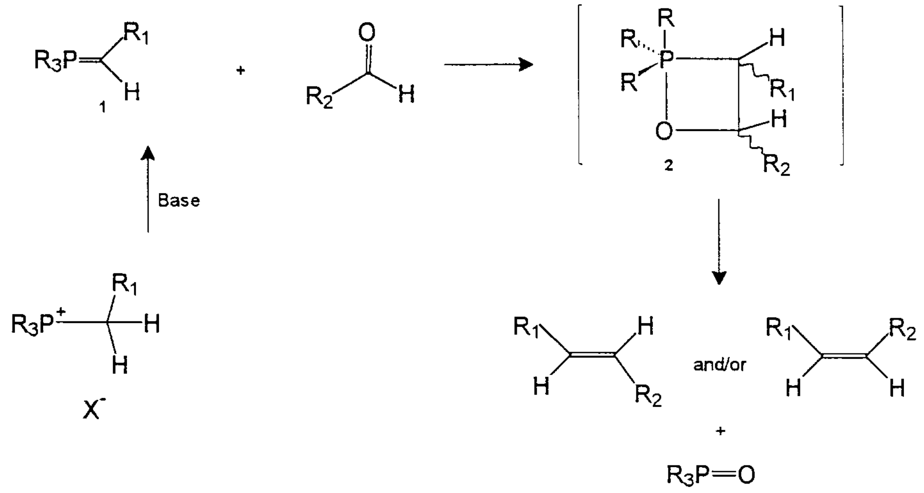

SCHEME 1 The Wittig olefination reaction.

philic attack of an alkyl or phenyl P-substituted phosphorus ylide on an aldehyde or ketone to form an alkene (or a mixture of geometrically isomeric alkenes) and a phosphine oxide (**4**). The reaction path that leads to the products is thought to proceed through two main steps: the formation of an oxaphosphetane intermediate (we have previously referred to this process as the Wittig half-reaction) and the decomposition of the oxaphosphetane to form the products [3]. It has been found experimentally that the formation of the oxaphosphetane determines the stereoselectivity of the reaction [4]. The stereoselectivity of the Wittig reaction is dependent on several factors [2b] such as the nature of the substituents on the phosphorus atom, the ylidic carbon, the carbonyl group, and the experimental conditions, such as ionic strength of the media, base utilized, presence of additives and catalyst, solvent polarity, concentration, pressure, and temperature.

The Wittig reaction of stabilized ylides (Scheme 1, R_1 = CN, COOR) with aldehydes is remarkably *E*-stereoselective [2,3]. Although the *E*-stereoselectivity can be readily rationalized in terms of the faster formation of the thermodynamically more stable *E*-oxaphosphetanes, this behavior is in contrast to the unusual *Z*-stereoselectivity observed in reactions of unstabilized ylides (R_1 = alkyl in Scheme 1). The *E*-stereoselectivity of the Wittig reaction of stabilized ylides is not greatly affected by experimental conditions, such as the presence of soluble metal ions, changes of reaction temperature, and concentrations of the reactants [2,3]. However, substituents on the phosphorus atom and the solvent employed have a pronounced effect on the yields of these reactions; i.e., replacement of the usual phenyl groups on the phosphorus atom of the ylide by alkyl groups promotes the Wittig reaction with less electrophilic aldehydes or even ketones and also increases the already marked *E*-stereoselectivity; under other circumstances, these aldehydes and ketones would be relatively unreactive [2,3]. Thus, stabilized P-phenyl substituted ylides, by far the most common case for the Wittig reaction, are highly *E*-stereoselective, whereas the corresponding unstabilized ones are highly *Z*-stereoselective. This observation suggests that the reaction profiles of these two different types of ylides are essentially different; i.e., for unstabilized ylides, oxaphosphetane formation is fast, and the rate-determining step of the reaction is the oxaphosphetane decomposition, whereas oxaphosphetane formation is slow and rate determining in the Wittig reaction of stabilized ylides. However, there might be a small possibility that oxaphosphetanes are not stable intermediates in the Wittig reaction of stabilized ylides.

The Wittig reactions of semistabilized ylides (Scheme 1, R_1 = phenyl, propargyl, vinyl, $-$F) represent a more complex situation. Wittig reactions of semistabilized P-phenyl substituted ylides with aldehydes may be either highly *Z*-stereoselective or highly *E*-stereoselective, depending on the conditions under which the reaction is carried out [2,3]. The presence of soluble Li^+ or Na^+ ions tends to increase the stereoselectivity ratios of *Z*/*E* up to as high as 90/10, whereas, under salt-free conditions, for the same reaction, the *Z*/*E* ratios are about 30/70 [5,6]. Furthermore, under salt-free conditions, as the polarity of the solvent employed is increased, the reaction of semistabilized ylides with aldehydes tends to yield higher *Z*/*E* ratios [2b,3]. As in the case of Wittig reactions of stabilized ylides with aldehydes, oxaphosphetanes have not been unambiguously identified as intermediates in the reactions of semistabilized ylides [7]. The same explanation given above for the case of stabilized ylides is also conceivable here, to explain the lack of oxaphosphetane detection. As in all Wittig reactions, the presence of alkyl substituents on the phosphorus atom brings about *E*-stereoselectivity in the Wittig reaction of semistabilized ylides with aldehydes. In general terms, the experimental variables (such as the nature of the solvent, temperature, concentration of the reactants, presence of soluble metal ions, and the base employed to effect deprotonation of the phosphonium cation) have dramatic effects on the *Z*/*E* ratios of alkenes produced in the Wittig reaction of semistabilized ylides with aldehydes [2,3].

Several mechanisms have been considered to explain the observed stereoselectivity of the Wittig reaction [2b,3]. However, particular attention has been given to the case of phenyl P-substituted unstabilized ylides. In general, two fundamental types of mechanisms have been proposed for oxaphosphetane formation: a one-step concerted cycloaddition and several versions of step-wise mechanisms that include ionic intermediates such as betaines and spin-paired dirradicals [2b,3]. Regardless of the reaction path that leads to oxaphosphetane formation, once formed, this intermediate undergoes pseudorotation about the phosphorus atom. This process places the oxygen atom in an equatorial position of the trigonal bipyramidal geometry formed around the phosphorus atom. Subsequent to pseudorotation, decomposition of the oxaphosphetane, which has been proposed to proceed either through an ionic or as a one-step mechanism [2b,3], leads to the alkene and the phosphine oxide.

This general pathway for the mechanism of the Wittig reaction requires refinement to accommodate the vast amount of experimental evidence accumulated through the years. Several issues concerning the intricate details for each step, for each type of reactants, or reaction conditions are subjects of intensive debate. Part of the problem is the lack of information concerning the nature of the transition states or transient intermediates that might be present in the Wittig reaction. Several theoretical studies have been undertaken in order to provide an insight on this matter [10–18]. For the most part, these studies make use of the mythical Wittig reaction [10,11,13–15,18] (the reaction of methylidenephosphorane with formaldehyde) to model this olefination process. We have recently found, using highly correlated ab initio methods, that this particular model reaction is unsuitable to describe the Wittig reaction [1]. Instead, alkyl-substituted phosphoranes, such as methylidenetrimethylphosphorane ($Me_3P=CH_2$), are required as a minimalist model for the appropriate description of the olefination process. In this article, we describe a comparative analysis of the reaction paths of trimethyl-P-substituted unstabilized, semistabilized, and stabilized ylides with acetaldehyde. We have studied the full reaction path (oxaphosphetane formation and decomposition) at the ab initio (MP2//HF/6-31G* and MP2/6-31G*) and semiempirical (MNDO-PM3) levels of theory. We have already established that these two methods represent the best compromise between the computational expense and the degree of rigor for the proper modeling of the Wittig reaction [1,15].

METHODOLOGY

The model reactions selected for the present study are shown in Scheme 2. These reactions correspond to those of the ylides ethylidenetrimethylphosphorane ($Me_3P=CH–Me$), propargylidenetrimethylphosphorane ($Me_3P=CH–C≡CH$), and cyanomethylidenetrimethylphosphorane ($Me_3P=CH–C≡N$) with acetaldehyde to form the respective *Z* and *E* oxaphosphetanes.

This first oxaphosphetane (oxa1) bears the oxygen atom in an axial position to the pentagonal bipyramidal geometry around the phosphorus atom (oxa1). This first oxaphosphetane will undergo pseudorotation to form the second oxaphosphetane (oxa2), by placing the oxygen atom in an equatorial position to the phosphorus atom. The second oxaphosphetane will undergo decomposition to form the products (the respective *Z* and *E* alkenes and trimethylphosphine oxide). These reactions are used as models to describe the reaction paths for unstabilized, semistabilized, and stabilized ylides and to explain mechanistically the experimental observations for the overall olefination reaction.

All geometry optimizations and energy calculations at the ab initio level were carried out using the Gaussian 94 suite of programs [19]. Reactants, intermediates, transition states, and products were fully optimized with the 6-31G* basis set at the Hartree-Fock (HF) level of theory. MP2/6-31G* single-point calculations on the HF geometries where used to compute the energetics of all reactions under study. The accuracy of these single-point computations was verified by comparing them with MP2 (full) calculations on model reaction 1a where fully optimized geometries were obtained at this level of theory (Scheme 2).

The geometrical optimizations for all model reactions were performed using the Berny optimization algorithm [20]. Reaction paths were computed by using eigen-following techniques, as well as the

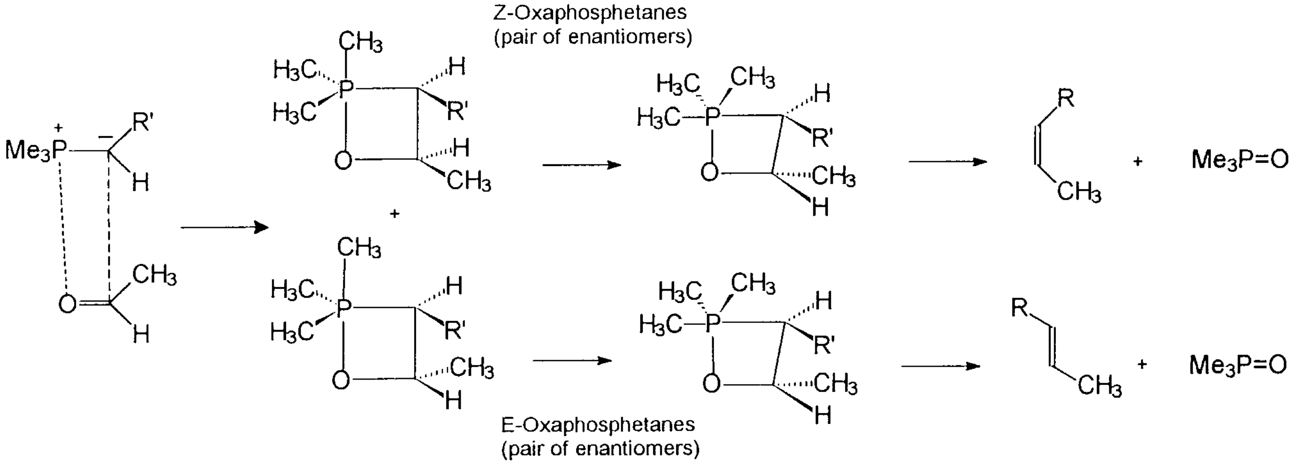

Reaction	**R**
1a(Z)	$-CH_3$
1b(E)	$-CH_3$
2a(Z)	$-C\equiv C-H$
2b(E)	$-C\equiv C-H$
3a(Z)	$-C\equiv N$
3b(E)	$-C\equiv N$

SCHEME 2 Model Wittig reactions for the study of the reactions of unstabilized, semistabilized, and stabilized with acetaldehyde.

IRC method developed by Gonzalez and Schlegel [21]. Analytical second derivatives were used to compute harmonic vibrational frequencies. These frequencies were used to characterize the stationary points as minima or saddle points. MP2 zero-point energy corrections were also computed and used to obtain the energetics of the reaction. The Wiberg bond indices [22] were calculated using the NBO-Read option implemented in Gaussian 94 as the squares of the bond indices. Another bond index analysis was carried out by the use of the relative variation of bond indices at the transition state of particular bonds i: δB_i[23], a parameter that is defined in equation 1:

$$\delta B_i = (B_i^{TS} - B_i^{R}) / (B_i^{R} - B_i^{R}) \tag{1}$$

where TS, R, and P refer to the transition state, reactant and product stages, respectively. An average value of these relative bond indices (δB_{av}), can be used as a measure of the degree of advancement of the transition state along a reaction path [23].

The AMSOL [24] (ver. 5.4) molecular orbital package utilizing the MNDO-PM3 Hamiltonian [25] was used for the semiempirical MO calculations. The transition states were located using the TSTATE option implemented in the same program. The systems were characterized as transition states by the presence of one negative force constant in the Hessian matrix of a force calculation [26].

All calculations (ab initio and semiempirical) were carried out on DEC Alpha AS/600 333MHz computers at the Multidisciplinary Research Computer Facility at Florida Atlantic University.

RESULTS AND DISCUSSION

Reaction Path

At all levels of theory (ab initio and MNDO-PM3), the Wittig reactions of ylides 1–3 are predicted to be a multistep process, where the first step is the formation of an adduct, which subsequently undergoes cycloaddition to form the first oxaphosphetane (oxa1). The second step is pseudorotation around the phosphorus atom leading to the second oxaphosphetane (oxa2). Decomposition of the second oxaphosphetane yields the products. The reaction path includes three intermediates (the adduct, oxa1, and oxa2) and three intrinsic barriers, one associated with the formation of oxa1, the second one associated with the formation of oxa2, and the third linked to the decomposition of oxa2 to form the products. Figure 1 shows the calculated energy profiles at the HF/6-31G*, MP2/6-31G*//HF/6-31G*,

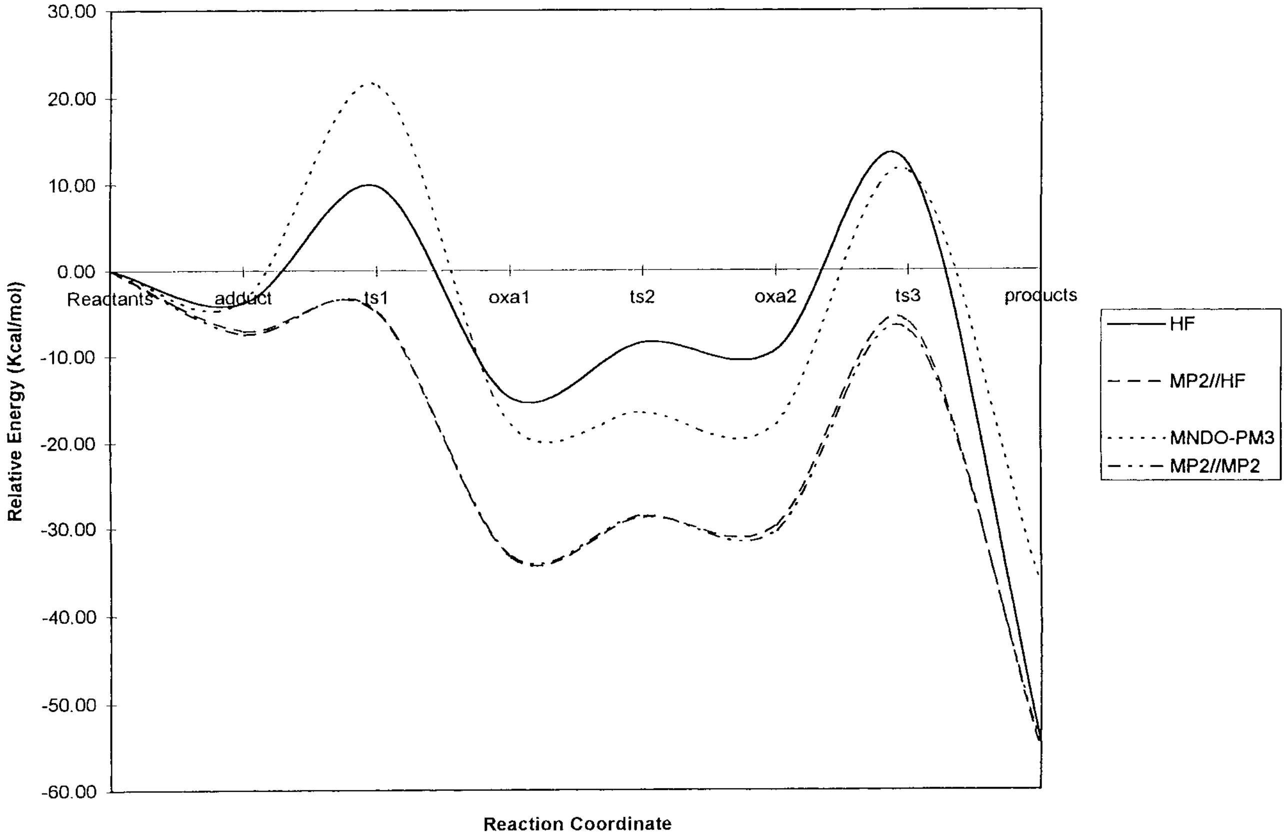

FIGURE 1 Reaction path profile at different levels of theory for **1a.**

MP2/6-31G*//MP2/6-31G*, and MNDO-PM3 for the reaction of ethylidenetrimethylphosphorane ($Me_3P{=}CH–CH_3$) with acetaldehyde to form *cis*-butene and trimethylphosphine oxide.

Significant differences in the relative energy levels of the intermediates and transition states can be observed with the different levels of theory. HF and MNDO-PM3 predict the first barrier to be too high when compared with MP2. The second and third barriers are comparable at all levels of theory; however, the calculated energies for oxa1 and oxa2 are higher at the HF and MNDO-PM3 levels. The same trend is observed for the model reaction that yields *trans*-butene (**1b**) and the other model reactions for semistabilized (**2a** and **2b**) and stabilized ylides (**3a** and **3b**).

It can be noticed from Figure 1 that the agreement between the MP2/6-31G*//HF/6-31G* and MP2/6-31G*//MP2/6-31G* profiles is quite remarkable. This is in accord with our previous findings [1], where HF calculations, though untenable for computing reliable energies, yield good geometries for the reaction profile of the Wittig half-reaction (the formation of oxa1). Therefore, single-point MP2 calculations on the HF geometries are sufficient to provide a high-quality reaction profile without incurring the exorbitant computational expense required for the full optimization using MP2.

Figure 2 shows the energy profiles of the three *Z*-generating model reactions (**1a, 2a,** and **3a**) used in this study at the MP2/6-31G*//HF/6-31G* level. The results depicted in Figure 2 show that the reaction profiles for these three ylides are qualitatively similar; all three reactions have three main intermediates (the adduct, oxa1, and oxa2), and three intrinsic barriers, with the interconversion of the oxaphosphetanes being the lowest. Similar profiles are obtained for the *E*-generating reaction (**1b, 2b,** and **3b**). Table 1 shows the energetics of the reactions of ylides 1, 2, and 3 with acetaldehyde.

It is interesting to notice that the barriers for the Wittig half-reaction leading to the formation of the Z-oxaphosphetane are between 1.4 and 4.7 kcal/mole higher than their *E*-generating counterparts (**1b–3b**). About the same energy differences are found between each *Z*-oxaphosphetane and *E*-oxaphosphetane. These observations denote a behavior that is in complete accordance with the Hammond postulate

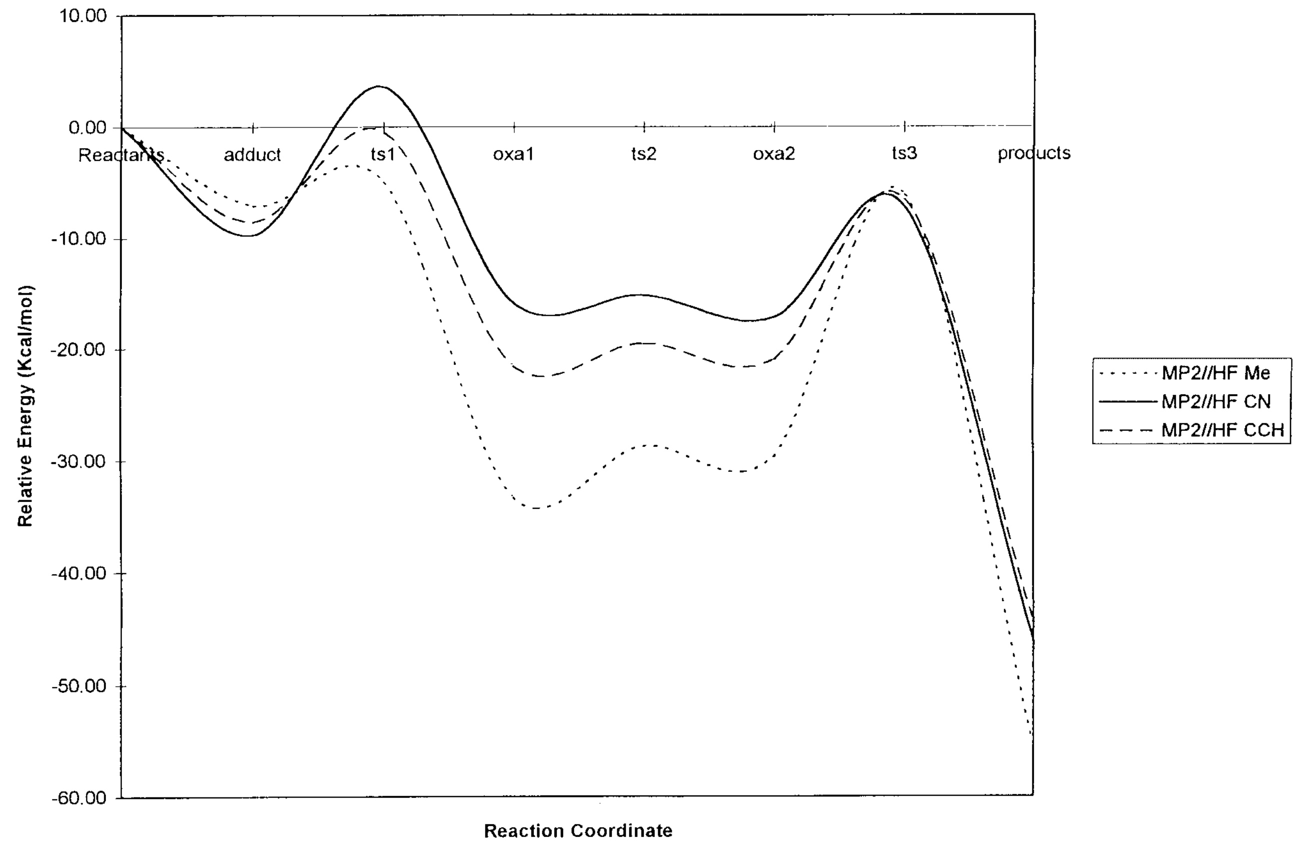

TABLE 1 MP2//HF Relative Energies (in Kcal/mol) of the Reactions of Unstabilized, Semistabilized, and Stabilized Ylides with Acetaldehyde[a]

Ylide	*Isomer*	*Adduct*	*Barrier*[b]	*oxa1*	*Barrier*[b]	*oxa2*	*Barrier*[b]	*Products*
Me	*cis*	−7.14	2.22(−4.92)	−33.32	4.52(−28.80)	−29.80	23.72(−6.09)	−55.30
	trans	−4.48	−2.44(−6.92)	−34.94	4.89(−30.05)	−31.15	24.30(−6.85)	−56.99
CCH	*cis*	−8.65	8.22(−0.44)	−21.51	1.89(−19.62)	−21.10	14.57(−6.53)	−44.16
	trans	−8.12	6.15(−1.97)	−22.45	3.17(−19.28)	−21.62	15.08(−6.53)	−44.13
CN	*cis*	−9.76	13.42(3.66)	−15.88	0.69(−15.19)	−17.21	10.04(−7.17)	−46.02
	trans	−9.69	12.03(2.34)	−16.72	−0.58(−17.30)	−17.44	10.14(−7.29)	−46.04

[a] All calculations were carried out using the 6-31G* basis set and ZPE corrections at the HF/6-31G* level.

[b] Numbers in parentheses are the relative energies of the transition states with respect to the reactants.

for reaction paths [27]. By way of contrast, the energy barriers for the interconversion of oxa1 into oxa2 are slightly higher (from 0.37 to 1.28 kcal/mol) for the *E*-oxaphosphetane than for their respective *Z* counterparts.

Geometries

Figure 3 shows the calculated geometries (HF/6-31G*) of the reactants (adduct), intermediates (oxa1 and oxa2), transition states (ts1, ts2, and ts3), and products (alkene and phosphine oxide) for the reaction of ethylidenetrimethylphosphorane ($Me_3P=CH{-}CH_3$) with acetaldehyde to form *trans*-butene and trimethylphosphine oxide. The relevant geometrical parameters for the other model reactions (**1a**, **2**, and **3**) are given in Table 2. Bond distances and bond indices for the relevant atom pairs associated with these geometries are shown in Table 2. As we have recently found [1], the formation of the adduct is due to electrostatic interactions between the ylide and the dipole in the aldehyde. There

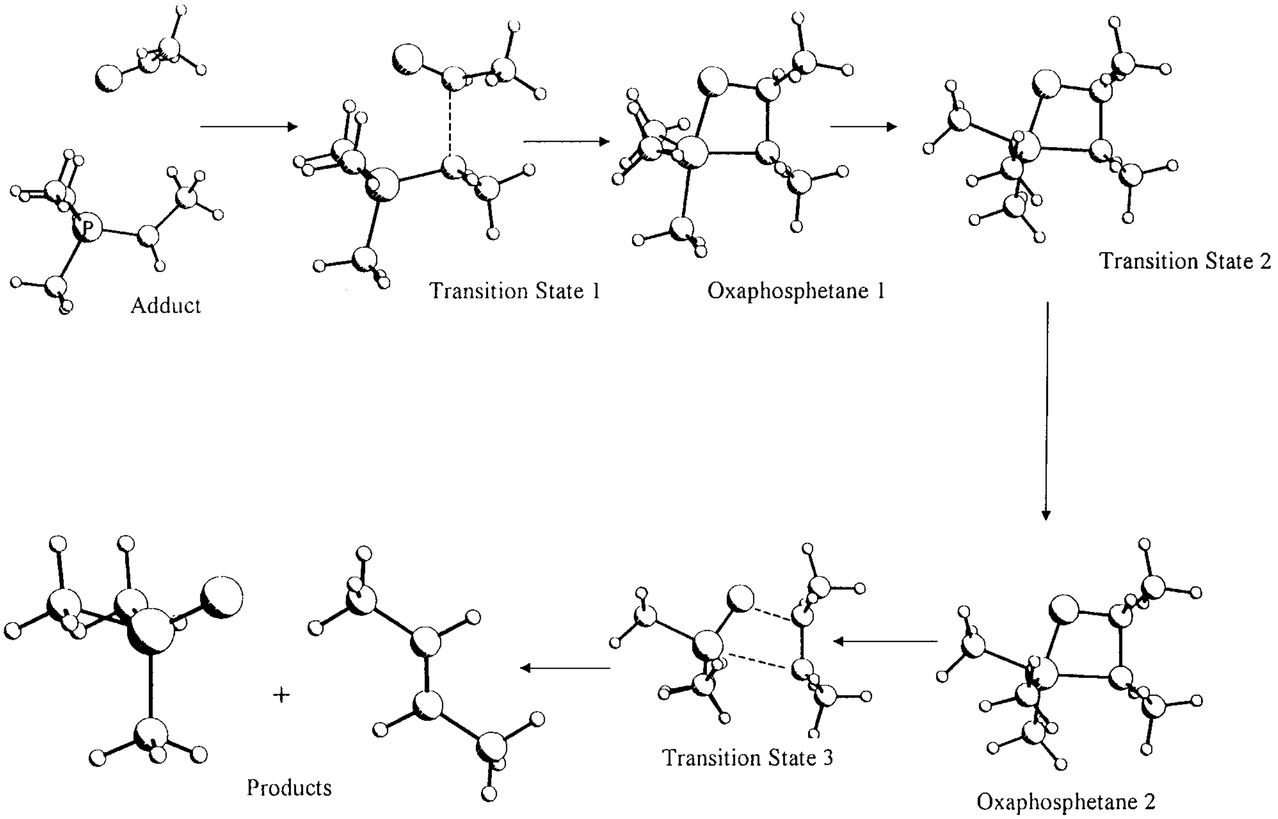

FIGURE 3 Calculated geometries (HF/6-31G*) of the reactants (adduct), transition states, intermediates (oxaphosphetanes), and products (trimethyl phosphine oxide and *trans*-butene) for the reaction of ethylidenephosphorane ($Me_3P=CH–CH_3$) with acetaldehyde.

is no evidence of covalent bonding between the reacting fragments at this stage (see below). The adduct then proceeds to form a transition state, which will acquire a cycloaddition-like (oxaphosphetane-like) geometry. However, this is an early transition state wherein the C–C bond distance is 2.11 Å with a corresponding bond index of 0.43. There is no evidence of covalent P–O bond formation as the bond index for this atom pair is 0.01, and the bond distance is 3.06 Å. At this stage, the phosphorus atom maintains an sp^3 hybridization tetragonal geometry. This first transition state (ts1) leads to the formation of the first oxaphosphetane (oxa1) which has a distorted pentagonal geometry around the phosphorus atom, and the oxygen atom occupies an axial position of the trigonal bipyramidal structure. This oxaphosphetane undergoes pseudorotation to form its isomeric counterpart (oxa2); in which the oxygen occupies an equatorial position of the trigonal bipyramidal structure around the phosphorus atom. This pseudorotation process occurs through the second transition state along the path (ts2) and essentially involves rearrangement of all ligands attached to the phosphorus atom. As the first oxaphosphetane (oxa1) undergoes pseudorotation, the P–O bond distances decrease from 1.82 to 1.69 Å, whereas the bond indices increase from 0.41 to 0.60 (Table 2). These changes indicate an increase in the bond P–O strength, a requirement for the advancement of the reaction toward the formation of the phosphine oxide.

The second oxaphosphetane (oxa2) undergoes a one-step decomposition to form *cis*-butene and trimethylphosphine oxide. This transformation proceeds through a transition state (ts3) in which it appears that breakage of the P–C (bond index 0.17) is very advanced when compared to the C–O breakage (bond index 0.46). This process can be described as a very asynchronous retrocycloaddition (borderline two-step mechanism). The nature of this transition state is reminiscent to ts1 in the sense that the highly polar nature of the species involved (mostly ionic in nature) affects the synchronicity of the reaction.

Similar reaction paths were obtained for the corresponding model reactions of the *E*-generating alkene derived from the reactions of the semistabilized and stabilized ylides (*E* and *Z*-generating alkenes). The geometries of the first transition state (ts1) of

TABLE 2 Wiberg Bond Indices and Geometrical Parameters for the Species Involved in the Model Reactions of Me$_3$P$=$CH$_2$ (**1a** and **1b**), Me$_3$P$=$CH–C≡CH (**2a** and **2b**), and Me$_3$P$=$CH–C≡N (**3a** and **3b**) with Acetaldehyde

	C–O		*C–P*		*C–C*		*P–O*		*<OCCP (degrees)*
	Distance	*Wiberg*	*Distance*	*Wiberg*	*Distance*	*Wiberg*	*Distance*	*Wiberg*	
Reaction **1a** *(Z-generating)*									
Reactants	1.19	1.84	1.66	1.31					
Add	1.19	1.79	1.69	1.26	3.51	0.01	3.97	0.00	−0.39
Ts1	1.24	1.41	1.76	1.03	2.10	0.44	3.03	0.01	15.16
Oxa1	1.39	0.93	1.87	0.82	1.54	0.99	1.81	0.41	5.84
Ts2	1.42	0.86	1.96	0.68	1.53	1.01	1.68	0.59	6.53
Oxa2	1.42	0.86	1.96	0.67	1.53	1.01	1.68	0.60	6.16
Ts3	1.72	0.46	2.62	0.18	1.43	1.28	1.55	0.84	2.48
Products					1.32	1.95	1.47	1.15	
Reaction **1b** *(E-generating)*									
Adduct	1.19	1.81	1.67	1.29	4.75	0.00	4.11	0.00	9.33
Ts1	1.24	1.42	1.75	1.03	2.11	0.43	3.06	0.01	7.84
Oxa1	1.39	0.93	1.87	0.82	1.53	0.99	1.82	0.41	−11.44
Ts2	1.42	0.87	1.96	0.69	1.52	1.01	1.69	0.58	−4.61
Oxa2	1.42	0.86	1.96	0.67	1.52	1.01	1.68	0.60	−10.11
Ts3	1.72	0.46	2.62	0.17	1.43	1.28	1.55	0.84	2.29
Products					1.32	1.95	1.47	1.15	
Reaction **2a** *(Z-generating)*									
Reactants	1.19	1.84	1.68	1.18					
Adduct	1.19	1.78	1.70	1.18	3.47	0.01	3.87	0.00	9.30
Ts1	1.26	1.32	1.78	0.95	1.95	0.54	2.88	0.01	−19.70
Oxa1	1.39	0.93	1.88	0.80	1.55	0.97	1.80	0.42	5.58
Ts2	1.41	0.87	1.97	0.65	1.53	0.99	1.70	0.56	−9.33
Oxa2	1.43	0.85	2.01	0.58	1.52	1.00	1.66	0.62	8.08
Ts3	1.59	0.60	2.73	0.11	1.46	1.16	1.55	0.80	2.04
Products					1.32	1.89	1.47	1.15	
Reaction **2b** *(E-generating)*									
Adduct	1.19	1.79	1.70	1.15	3.41	0.01	3.90	0.00	−16.61
Ts1	1.26	1.34	1.78	0.96	1.96	0.52	2.92	0.01	−25.98
Oxa1	1.39	0.93	1.88	0.78	1.54	0.97	1.81	0.42	−12.60
Ts2	1.41	0.88	1.97	0.67	1.53	0.99	1.71	0.56	−5.20
Oxa2	1.43	0.85	2.00	0.59	1.60	1.00	1.67	0.61	11.36
Ts3	1.59	0.60	2.75	0.10	1.32	1.89	1.47	1.15	−6.80
Products					1.32	1.89	1.47	1.15	
Reaction **3a** *(Z-generating)*									
Reactants	1.19	1.84	1.69	1.14					
Adduct	1.19	1.77	1.70	1.12	4.44	0.00	3.91	0.00	1.68
Ts1	1.27	1.28	1.80	0.92	1.88	0.60	2.81	0.02	−21.17
Oxa1	1.39	0.93	1.89	0.76	1.54	0.97	1.80	0.43	5.90
Ts2	1.41	0.89	1.96	0.66	1.53	0.99	1.72	0.54	−10.39
Oxa2	1.43	0.84	2.07	0.52	1.52	1.00	1.64	0.65	4.98
Ts3	1.54	0.66	2.72	0.11	1.47	1.11	1.56	0.78	2.48
Products					1.32	1.88	1.47	1.15	
Reaction **3b** *(E-generating)*									
Adduct	1.19	1.77	1.70	1.12	4.47	0.00	3.91	0.00	−7.65
Ts1	1.26	1.30	1.79	0.93	1.90	0.57	2.85	0.02	−28.21
Oxa1	1.39	0.93	1.89	0.75	1.54	0.97	1.80	0.42	−13.02
Ts2	1.41	0.89	1.95	0.67	1.53	0.99	1.72	0.53	−14.52
Oxa2	1.43	0.84	2.07	0.52	1.52	1.00	1.64	0.64	7.60
Ts3	1.54	0.66	2.73	0.11	1.47	1.11	1.56	0.70	4.73
Products					1.32	1.88	1.47	1.15	

our model reactions (*Z*-generating isomer) are depicted schematically in Figure 4. All atoms that participate in the bond breaking–forming process (P, C, C, and O) are essentially in the same plane. However, a slight degree of puckering (measured in terms of the <PCCO dihedral angle) that varies between −0.39° and −28.21° (Table 2) is found for most of these transition states. The largest degree of puckering is observed for the reaction of stabilized ylides. The forming C–C bond distances found in the transition state in these model reactions was 1.88 Å for the $Me_3P{=}CH{-}CN$ case, 1.95 Å for the $Me_3P{=}CH{-}C{\equiv}CH$ case, and 2.10 Å for the $Me_3P{=}CH{-}CH_3$ case. On the other hand, the P–O bond distances are significantly longer for these transition states as distances of 2.81, 2.88, and 3.03 Å are found for the reactions of stabilized, semistabilized, and unstabilized ylides, respectively.

Energetics

The first intrinsic barrier of activation of the Wittig half-reactions of the ylides with acetaldehyde increases steadily from 2.22 kcal/mole for the case of the unstabilized ylide to 13.42 kcal/mole for the stabilized ylide (Table 1). This trend clearly indicates that, as the carbanionic charge on the ylidic carbon is delocalized by the attached substituents, the reactivity of the ylide is decreased accordingly. These ab initio results predict the experimentally observed reactivity of these ylides according to the nature of the substituents attached to the ylidic carbon.

An analysis of the energetics of formation of the oxaphosphetanes indicates that, as the substituents on the ylidic carbon range from alkyl groups (unstabilized ylides) to cyano (stabilized ylides), the heat of reaction of the Wittig half-reactions becomes less negative. Therefore, as observed in the case of the reaction profiles of the Wittig half-reaction of unstabilized ylides with aldehydes of different electrophilicity [17], the reactions of acetaldehyde with ylides of different stability follow a "Hammond-like" behavior [27], since the reactions with the higher energy of activation are the least favorable thermodynamically.

The opposite behavior is found for the decomposition of the second oxaphosphetane (oxa2) to form the products. In this case, the barriers of activation decrease steadily from 24.30 kcal/mole for the case of unstabilized ylides to 10.04 kcal/mole for the stabilized ylides (Table 1). However, the relative energy of the products (the alkene and trimethylphos-

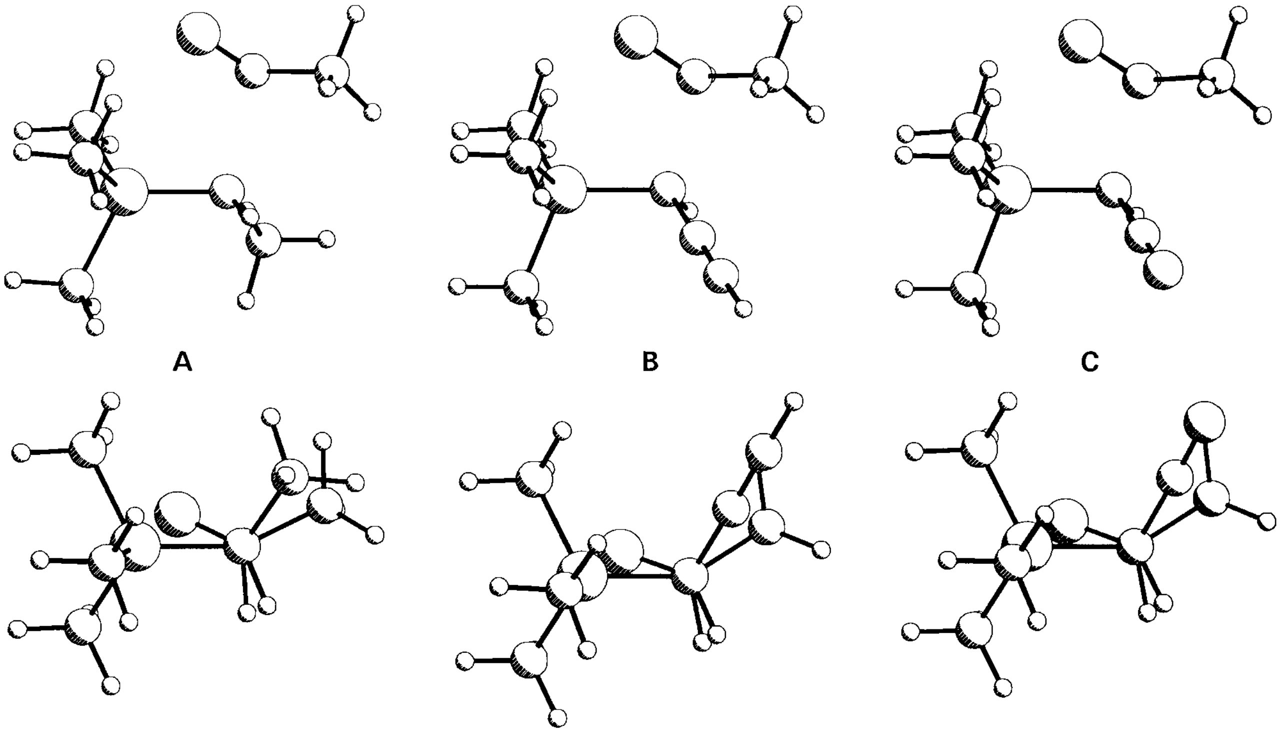

FIGURE 4 Geometries of the first transition states (*Z*-generating) of the reaction of (A) unstabilized, (B) semistabilized, and (C) stabilized ylides with acetaldehyde. The upper view places the P, C, C, and atom in the plane of the paper. The lower view places these atoms in a plane perpendicular to the paper, showing the degree of puckering exhibited by the PCCO dihedral angle.

phine oxide) are the most negative for the case of the reaction of unstabilized ylides (−56.99 kcal/mole), followed by the reaction of stabilized ylides (−46.04 kcal/mole), and then for the reaction of semistabilized ylides (−44.16 kcal/mole).

An analysis of the energy barriers depicts a process that can be described as follows: in all cases, it is predicted that the rate-determinant step of the reaction is the decomposition of the second oxaphosphetane (oxa2). This barrier is highest for the reaction of unstabilized ylides. This is in accord with the fact that oxaphosphetanes are detectable intermediates for the Wittig reaction of unstabilized ylides. In the case of semistabilized and stabilized ylides, the barrier for the formation of the oxaphosphetane is comparable to the decomposition barrier; this might explain why the oxaphosphetanes of these ylides have escaped spectroscopic detection. The barrier for the interconversion of oxaphosphetanes is relatively small (<5 kcal/mol). It has been already determined that oxaphosphetane pseudorotation plays a secondary role in the overall mechanism of the Wittig reaction [28].

According to the arguments presented before, it would be expected that, as the Wittig half-reaction becomes less favorable thermodynamically, the transition state (ts1) would tend to be more advanced in the reaction path or more "oxaphosphetane-like." Issues regarding the advancement and synchronousness of the Wittig half-reaction are better dealt with by use of bond index analyses as previously shown [1,15,17]. A detailed analysis of the calculated bond indices of our model Wittig reactions will now be presented.

Table 2 shows the bond indices and their respective bond distances of the atom pairs involved in the bond breaking–forming process for reactions 1–3. The following common features can be found between the bond index analyses of all these model reactions:

1. No major differences at any stage of the reaction paths were detected between the bond indices of reactions that generate the *Z*-stereoisomers and those that generate the *E*-stereoisomers. Thus, along the whole reaction path, both types of reactions (*Z*-generating and *E*-generating) have about the same degree of advancement in the bond breaking–forming processes in the transition states.
2. In all cases, the C–C bond is more than 40% formed at the transition state. The results of bond index calculations (absolute, relative, or average) for the reactions of unstabilized ylides (reaction 1) as compared with those of the reactions of semistabilized (reaction 2) and stabilized ylides (reaction 3), show that the latter reactions are more advanced (i.e., have a later transition state). This is reflected in the percentages of C–C bond formation at the transition states; 44% in the case of reaction 1 (R′ = −CH3), 54% for reaction 2 (R′ = −C≡CH), vs. up to 60% for reaction 3 (R = −C≡CN).
3. The bond index analyses reveal the behavior of bond strengths within individual atom pairs throughout the reaction path of these model Wittig reactions. Thus, the P–C and C–O bond strengths decrease as the reaction proceeds, whereas the C–C and P–O bond strengths increase.

Other significant differences in the bond indices analyses between the model Wittig reactions of unstabilized ylides with acetaldehyde and the model reactions of semistabilized and stabilized ylides are found in the third transition state (ts3). In the case of the model reaction of unstabilized ylides, the P–C bond index is about 0.18 at the ts3 stage, whereas in the case of semistabilized and stabilized ylides, the P–C bond orders are about 0.11. Likewise, the C–O bond indices are markedly different (about 0.46 for the reactions of unstabilized ylides, and 0.60 and 0.66 for the reaction of semistabilized and stabilized ylides, respectively). Only small differences can be found in the bond indices and distances for the P–O and C–C atom pairs. A rationalization for such behavior in the bond indices can be attempted by consideration of the possible structural differences of these transition states as depicted in Scheme 3.

Structures **D** and **E** make a greater contribution to the structure of ts3, which is the result of the reaction of a stabilized ylide, than does structure **B** to the ts3 obtained from the reaction of an unstabilized ylide. Similar arguments can be applied to ts3 derived from the reactions of the other stabilized ylides and also to those obtained from semistabilized ylides. Therefore, for third transition states (ts3) obtained from the reactions of stabilized and semistabilized ylides, P–C bond distances are expected to be longer and the C–O bond distances to be shorter than those of the ts3 of unstabilized ylides.

Additional insight into the energetics of the Wittig reactions of stabilized ylides with acetaldehyde (or any other suitable carbonyl compound) compared to the corresponding reactions of unstabilized ylides can be gleaned by examinations of the structures of the respective ylides. In this regard, the work of Schlosser et al. [29] is of importance. By use of

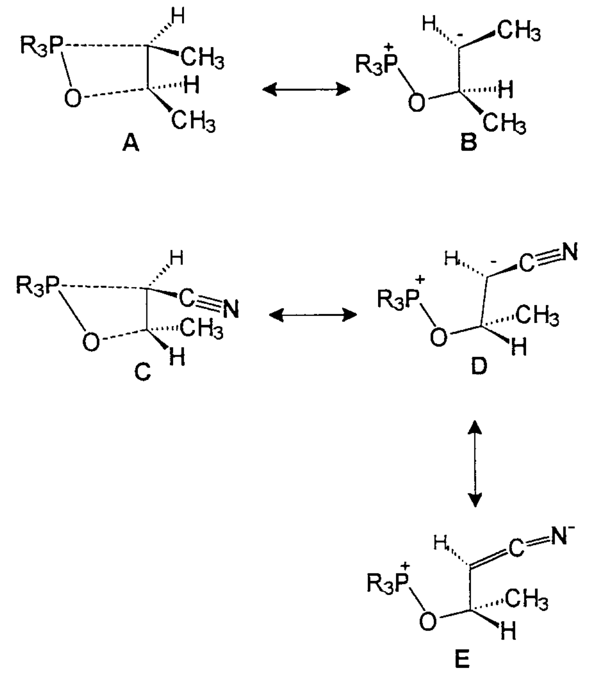

SCHEME 3 Possible resonance structures of the third transition (ts3) of the Wittig reaction of unstabilized and stabilized ylides.

^{13}C-chemical shifts as a probe for the electronic environment of the α-carbon centers, these workers found that, for triphenylphosphoniomethylide, a model case for an unstabilized ylide, the Zwitterion structure **H** is the dominant contributing resonance structure, and the P–C double bond structure **I** is a higher-energy (minor) contributing structure. These experimental findings concur with the theoretical predictions reported by Bachrach [30] using ab initio calculations at the MP2 level and basis sets larger than 6-31G*:

$$\underset{\mathbf{H}}{\phi_3\overset{+}{P}\text{–}\overset{-}{C}H_2} \leftrightarrow \underset{\mathbf{I}}{\phi_3P=CH_2}.$$

For triphenylphosphonio-propenide, a typical semistabilized ylide, resonance structure **J** is the main contributor to the hybrid, and **K** and **L** are minor contributing structures

$$\underset{\mathbf{J}}{\phi_3\overset{+}{P}\text{–}\overset{-}{C}H\text{–}CH=CH_2} \leftrightarrow \underset{\mathbf{K}}{\phi_3P=CH\text{–}CH=CH_2}$$

$$\leftrightarrow \underset{\mathbf{L}}{\phi_3\overset{+}{P}\text{–}CH=CH\text{–}\overset{-}{C}H_2}.$$

For (methoxycarbonylmethylene)triphenylphophorane, a typical stabilized ylide, roughly equal distribution of the negative charge is found on the α-carbon and the oxygen atom; i.e., the main contributing resonance structures are **M** and **yN,** while structure **O** is a minor contributing structure.

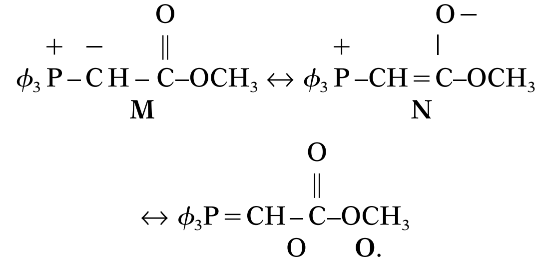

$$\underset{\mathbf{M}}{\phi_3\overset{+}{P}-\overset{-}{C}H-\overset{\overset{O}{\|}}{C}\text{–}OCH_3} \leftrightarrow \underset{\mathbf{N}}{\phi_3\overset{+}{P}\text{–}CH=\overset{\overset{O-}{|}}{C}\text{–}OCH_3}$$

$$\leftrightarrow \phi_3P=CH-\overset{\overset{O}{\|}}{C}\text{–}OCH_3$$
$$\mathbf{O}\quad \mathbf{O}.$$

These data fortify the already prevalent concept that the order of decreasing nucleophilicity of the α-carbon of ylides is

Unstabilized > Semistabilized > Stabilized.

Since methoxycarbonyl, cyano and similar groups are fundamentally electron-withdrawing in nature, it also follows that the electrophilicities of the phosphorus atom of ylides should exhibit the following decreasing order:

Stabilized > Semistabilized > Unstabilized.

According to our present ab initio results on Wittig reactions, initial carbon–carbon bond formation should contribute to the driving force of the reaction more in the reactions of unstabilized ylides than in those of stabilized ylides (with those of semistabilized ylides falling in between), although such bond formation is of major importance in all three cases. These comments apply to the first half of the Wittig reaction.

With regard to the second half of each Wittig reaction, the decomposition of the oxaphosphetane to the ultimate products (alkenes plus phosphine oxide) can be described as depicted in Scheme 4. The resonance stabilization of the transition state (**F** ↔ **G**) for the reaction of the oxaphosphetane derived from the stabilized ylide should lower the activation energy as against the analogous situation for the oxaphosphetane derived from the unstabilized ylide (again with the semistabilized case in between). Thus, the rates of decomposition of the respective oxaphosphetanes should follow the order

Stabilized > Semistabilized > Unstabilized.

If these considerations are valid, it is clear why oxaphosphetanes have not been experimentally observed in the Wittig reactions of semistabilized and stabilized ylides, with aldehydes: They decompose faster than they can be formed. On the other hand, in the reactions of unstabilized ylides with aldehydes, oxaphosphetanes are readily observed, because they form faster than they can decompose.

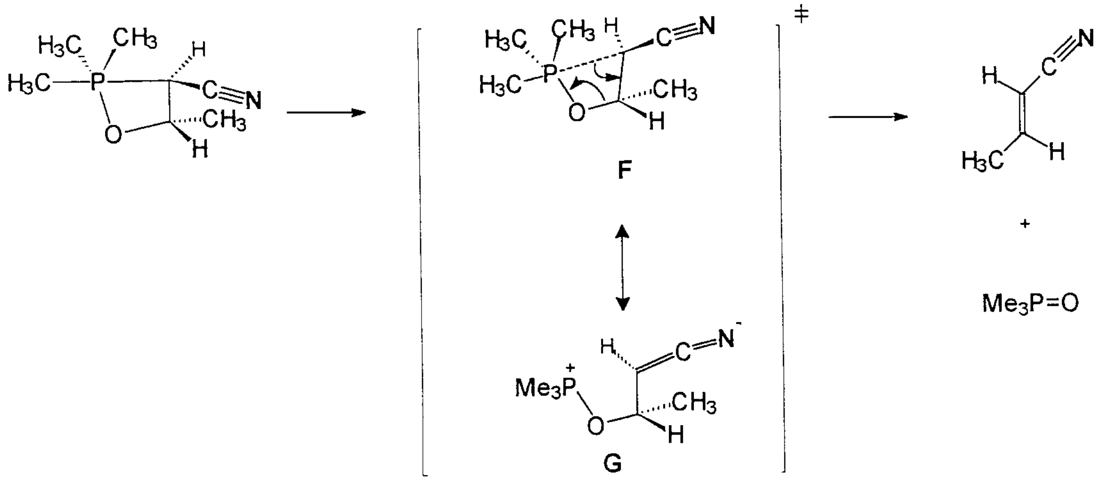

SCHEME 4 Possible mechanism for the oxaphosphetane decomposition in reactions of stabilized ylides with aldehydes.

The mechanism presented above is reminiscent of the one proposed by Bestmann to explain the stereoselectivity of the Wittig reaction[12]. According to Bestmann, the stereoselectivity determining step might occur with unstable intermediates of the type (**D** ↔ **E**), because bond rotation around the C–C bond in such intermediates is presumed to be faster than alkene elimination. Bestmann's mechanism has not been widely accepted to explain the steroselectivity of the Wittig reaction, and evidence has been gathered against it[2b,3]. The evidence, however, pertains to (**D** ↔ **E**) being intermediates rather than transition states, as we have proposed. Maryanoff et al.[4] have presented evidence that the stereoselectivity of the Wittig reaction is determined in the oxaphosphetane formation stage (the Wittig half-reaction) and not at the oxaphosphetane decomposition stage as suggested by Bestmann[12]. However, issues regarding the oxaphosphetane stability, and the mechanism of oxaphosphetane decomposition, have not been widely addressed in the past. The bond index analyses provided by applying correlated ab initio calculations to the oxaphosphetanes, as shown above, provide good evidence to support the oxaphosphetane decomposition pathway depicted in Scheme 3, which involves a transition state (**D** ↔ **E**) rather than an intermediate. Isotopic labeling experiments carried out by Vedejs et al.[28a] also rule out the possibility of formation of an intermediate such as (**D** ↔ **E**) but not a related transition state.

According to the evidence presented above, the transition states of the Wittig half-reactions of semistabilized and stabilized ylides still show the same important ionic character presented by the reactions of unstabilized ylides (Scheme 4).

The slightly shorter P–O bond distance is indicative that the first half of the reactions of semistabilized and stabilized ylides is more synchronous than in the reactions of unstabilized ylides.

The origin of the *E*-stereoselectivity of the Wittig reaction of unstabilized, semistabilized, and stabilized alkylidenephosphoranes correspond to the ones already shown at the MNDO-PM3 level for unstabilized ylides. For the first half of the reaction, a larger steric strain built into the reaction that leads to the *Z*-products, yields reaction paths that are less favorable than for those reactions that lead to the formation of the *E*-alkene. In this regard, the MO (ab initio and MNDO-PM3) calculations were able to predict the experimentally observed stereoselectivity. However, in the overall mechanistic scheme of the Wittig reaction, the main question remains only partially answered: What are the origins of the unusual *Z*-stereoselectivity of the reactions of alkylidenetriphenylphosphoranes with aldehydes? The main difference in the reaction paths between the reaction of unstabilized ylides with aldehydes and the reaction of stabilized ylides (and perhaps semistabilized ylides as well), is the degree of synchronousness of the reaction. The implications of such a difference in the mechanistic scheme of the Wittig reaction are being explored further as we are in the process of including phenyl groups as substituents on the phosphorus atom and the role of solvents in our model reactions.

ACKNOWLEDGMENTS

This work was supported in part by the National Science Foundation (CDA-9512266). The authors would like to thank the Science and Hispanity Foundation for a fellowship to (A.A.R.) Supplementary material available: the *Z* Matrix of the optimized molecular structures (contact the authors for a suitable media of data transferring).

REFERENCES

[1] (a) Molecular modeling of the Wittig reaction 6; (b) previous article in this series: A. A. Restrepo-Cossio, C. A. Gonzalez, F. Mari, in preparation.

[2] For recent reviews of the Wittig reaction, see (a) B. J. Walker, *Organophosphorus Chem. 27,* 1996, 264; (b) A. W. Johnson, *Ylides and Imines of Phosphorus,* Wiley, New York, (1993); (c) B. Maryanoff, A. E. Reitz, *Chem. Rev., 89,* 1989, 863.

[3] For recent reviews of the Mechanism and Stereoselectivity of the Wittig reaction, see (a) E. Vedejs, M. J. Peterson, *Top. Stereochem. 21,* 1994, 1; (b) E. Vedejs, M. J. Peterson, *Adv. Carbanion Chem. 2,* 1994, 1.

[4] B. E. Maryanoff, A. B. Reitz, M. S. Mutter, M. S. Inners, R. R. H. Almond, R. Whittle, R. R. Olofson, *J. Am. Chem. Soc. 108,* 1986, 7664.

[5] W. J. Ward, W. E. McEwen, *Phosphorus and Sulphur, 41,* 1989, 393.

[6] W. J. Ward, W. E. McEwen, *J. Org. Chem., 55,* 1990, 493.

[7] The observation of unusually stable oxaphosphetanes derived from one semistabilized[5] and one stabilized ylide[8] has recently been reported. In the semistabilized case, a dibenzophosphole substituted phosphorus atom in the oxaphosphetane is stabilized relative to the phosphine oxide product, hence the decomposition rate is retarded. In the stabilized case, resistance to oxaphosphetane decomposition is provided by the stabilizing effects of electron-withdrawing groups and ring strain on the phosphorus atom.

[8] E. Vedejs, T. J. Fleck, *J. Am. Chem. Soc., 111,* 1989, 5861.

[9] T. Kawashima, K. Kato, R. Okasaki, *Angew. Chem. Int. Ed. Engl., 32,* 1993, 869.

[10] C. Trindle, J. T. Hwang, F. A. Carey, *J. Org. Chem., 38,* 1973, 2664.

[11] R. Höller, H. Lischka, *J. Am. Chem. Soc., 102,* 1980, 4632.

[12] H. J. Bestmann, *Pure Appl. Chem., 52,* 1980, 771.

[13] F. Volatron, O. Eisenstein, *J. Am. Chem. Soc., 109,* 1987, 1.

[14] H. S. Rzepa, *J. Chem. Soc. Perkin Trans. II,* 1989, 2115.

[15] F. Mari, P. M., Lahti, W. E. McEwen, *Heteroatom Chem., 2,* 1991, 265.

[16] H. Yamataka, T. Hanafusa, S. Nagase, T. Kurakake, *Heteroatom Chem. 2,* 1991, 465.

[17] F. Mari, P. M. Lahti, W. E. McEwen, *J. Am. Chem. Soc., 114,* 1992, 813.

[18] T. Naito, S. Nagase, H. Yamataka, *J. Am. Chem. Soc., 116,* 1994, 10080.

[19] GAUSSIAN 94; M. J. Frisch, G. W. Trucks, H. B. Schlegel, P. M. W. Gill, B. G. Johnson, M. A. Robb, J. R. Cheeseman, T. Keith, G. A. Petersson, J. A. Montgomery, K. Raghavachari, M. A. Al-Laham, V. G. Zakrzewski, J. V. Ortiz, J. B.Foresman, J. Cioslowski, B. B. Stefanov, A. Nanayakkara, M. Challacombe, C. Y. Peng, P. Y. Ayala, W. Chen, M. W. Wong, J. L. Andres, E. S. Replogle, R. Gomperts, R. L. Martin, D. J. Fox, J. S. Binkley, D. J. Defrees, J. Baker, J. P. Stewart, M. Head-Gordon, C. Gonzalez, and J. A. Pople, Gaussian, Inc., Pittsburgh, PA (1995).

[20] H. B. Schlegel, *J. Comp. Chem., 3,* 1982, 214.

[21] C. A. Gonzalez, H. B. Schlegel, *J. Chem. Phys., 90,* 1989, 2154.

[22] K. B. Wiberg, *Tetrahedron, 24,* 1968, 1083.

[23] A. Moyano, M. A. Pericàs, E. Valentí, *J. Org. Chem., 54,* 1989, 573.

[24] AMSOL v5.4; G. D. Hawkins, G. C. Lynch, D. J. Giesen, I. Rossi, J. W. Storer, D. A. Liotard, C. J. Cramer, and D. G. Truhlar; Quantum Chemistry Program Exchange Program 606, based in part on AMPAC-version 2.1 by D. A. Liotard, E. F. Healy, J. M. Ruiz, and M. J. S. Dewar.

[25] (a) J. J. P. Stewart, *J. Compt. Chem., 10,* 1989, 209; (b) J. J. P. Stewart, *J. Compt. Chem., 10,* 1989, 221.

[26] J. W. McIver, A. Komornicki, *J. Am. Chem. Soc., 94,* 1972, 2625.

[27] G. S. J. Hammond, *J. Am. Chem. Soc., 77,* 1955, 334.

[28] (a) E. Vedejs, C. F. Marth, *J. Am. Chem. Soc., 111,* 1989, 1519; (b) E. Vedejs, C. F. Marth, *J. Am. Chem. Soc., 112,* 1990, 3105.

[29] M. Schlosser, T. Jenney, B. Schaub, *Heteroatom Chemistry, 1,* 1990, 153.

[30] S. Bachrach, *J. Org. Chem., 57,* 1992, 4367.